

Supplementary Information for

**Patched1-ArhGAP36-PKA-Inversin axis determines the ciliary  
translocation of Smoothed for Sonic Hedgehog pathway activation**

Boyan Zhang, Tenghan Zhuang, Qiaoyu Lin, Biying Yang, Xiaowei Xu, Guangwei Xin,  
Shicong Zhu, Gang Wang, Bin Yu, Tingting Zhang, Qing Jiang and Chuanmao Zhang\*

\*Correspondence should be addressed to: Chuanmao Zhang.

E-mail: zhangcm@pku.edu.cn

**This PDF file includes:**

Materials and Methods  
Figs. S1 to S9

## **Materials and Methods**

### **Antibodies and reagents**

Antibodies and reagents including SAG (Enzo, Cat. # ALX-270-426), cyclopamine (Tocris, Cat. # 1623), SANT1 (Sigma, Cat. # S4572), forskolin (Sigma, Cat. # F6886), H89 (Sigma, Cat. # B1427), 20 $\alpha$ -hydroxycholesterol (20-OHC, Sigma, Cat. # H6378); rabbit anti-ArhGAP36 (Atlas, Cat. # HPA002064), anti-IFT88 (Proteintech, Cat. # 13967-1-AP), anti-Gli1 (Cell Signaling, Cat. # 2534), anti-phosphor T198 PKA C $\alpha$  (Cell Signaling, Cat. # 4781), anti-Smo (Abcam, Cat. # ab38686), anti-Ptc2 (Lifespan, Cat. # LS-C312999), anti-SENP1 (Abcam, Cat. # ab108981), anti-CK1 $\gamma$ 1 (Rui Ying Biotechnology, Cat. # rlt0647), anti-GRK2 (Rui Ying Biotechnology, Cat. # rlt2064); goat anti-Inversin (Santa Cruz Biotechnology, Cat. # sc-8719), anti-Ptc1 (Santa Cruz Biotechnology, Cat. # sc-6149); mouse anti-Sufu (Santa Cruz, Cat. # sc-137014), anti-GFP (MBL, Cat. # M048-3), anti-PKA C $\alpha$  (Santa Cruz Biotechnology, Cat. # sc-28316), anti-EVC (Santa Cruz Biotechnology, Cat. # sc-271955), anti- $\gamma$ -tubulin (Sigma, Cat. # T6557), anti-c-Myc (Sigma, Cat. # M4439), anti-Flag (Sigma, Cat. # F1804), and acetylated  $\alpha$ -tubulin (Sigma, Cat. # T7451) were purchased from the indicated companies. Rabbit anti-phosphor-InversinT647 was produced using a KLH-coupled polypeptide GASQKRRT(p)HQLRDRCSPA corresponding to the amino acid sequence of mouse Inversin. All animal experiments were performed according to the approved guidelines.

### **Cell culture and synchronization**

The Ptc1<sup>+/-</sup>, Ptc1<sup>-/-</sup>, and Sufu<sup>-/-</sup> MEF cells were kind gifts from Drs. William E. Moerner, Ljiljana Milenkovic (Stanford University, USA), and Rune Toftgård (Karolinska Institutet, Sweden); the Kif3a<sup>-/-</sup> and Smo<sup>-/-</sup> MEF cells were kind gifts from Dr. Steven Y. Cheng (Nanjing Medical University, China); Wild-type MEF and HEK 293T cells were from American Type Culture Collection (ATCC). Cells were cultured at 37°C in Dulbecco's modified Eagle medium (DMEM) containing 10% fetal bovine serum under standard culture conditions, and were confirmed without mycoplasma contamination. Cells were arrested at the G0 phase by culturing for 36 hr in medium containing 0.5% serum.

### **Molecular cloning and gene knockdown with Crispr/Cas9 technology**

The constructs encoding the human ArhGAP36, Inversin and the mouse Ptc1 genes were kind gifts from Drs. Oliver Rocks (Max-Delbrueck Center for Molecular Medicine, Germany), Gerd Walz (University of Freiburg Medical Center, Germany) and Xiaoyan Zheng (The George Washington University, USA). The Crispr/Cas9 targeting sequences for mouse Inversin were #1 5'-

TGCACCTGAGCACTCGGCAC-3' and #2 5'-CGCTGATGGAAACCTAACGG-3'; for mouse ArhGAP36 were #1 5'-CACCGCCAGGACGCTCACACGGCGG-3' and #2 5'-CACCGGCTGGACTGCCTATTCGCAT-3'. The DNA fragments for expressing these sequences were generated by annealing the indicated pairs of oligonucleotides and ligating into the pSpCas9(BB)-2A-Puro vector (Origene, Cat. # PX459).

### **Transient transfection, lentivirus infection and stable cell-line establishment**

Transient cDNA transfections were carried out on cells using the MegaTran transfection reagent (Origene, Cat. # TT200002) for HEK 293T cells or using the lentivector expression system (System Biosciences) encoding the indicated genes for MEF cells, according to the manufacturers' instructions. To establish stable MEF cell-lines expressing the WT and T794A/D mutant GFP-Inversin, or the WT and K73H mutant GFP-PKAc, the cells were transfected with the indicated plasmids overnight, and neomycin (G418) was added to a final concentration of 500 µg/mL to the medium 48 hr post-transfection for stable cell-line selection. To establish stable Ptc1<sup>-/-</sup> cells expressing the full-length and truncated forms of Ptc1-GFP, Ptc1<sup>-/-</sup> cells were infected by lentivirus encoding the indicated DNA overnight, and puromycin was added to a final concentration of 1.5 µg/mL to the medium 48 hr post-transfection for stable cell-line selection.

### **Phosphorylation site prediction and *in vitro* kinase assay**

Prediction of Inversin phosphorylation site by PKA was carried out using Group-based Prediction System (GPS v2.1) with the threshold "medium". The wild-type full-length GFP-Inversin and its wild-type or T794A mutant fragments were immunoprecipitated from G0 phase HEK 293T cells. Beads coated with equal amounts of GFP-Inversin or its mutant were combined with the catalytic subunit of PKA kinase (NEB, Cat. # P6000). The reaction was supplemented with 10 µCi  $\gamma$ -<sup>32</sup>P ATP and incubated for 30 min at 30°C. Loading buffer was added to stop the reaction. After electrophoresis of samples by SDS-PAGE, the gel was exposed to X-ray film for 6 hr.

### **Luciferase reporter assay**

The firefly luciferase reporter driven by eight Gli1 binding sites (8×GliBS) was kindly provided by Dr. Yun Zhao (Shanghai Institute of Biochemistry and Cell Biology, China). The Smo<sup>W535L</sup> or Smo<sup>L412F</sup> Cells were each transfected with 0.5 µg 8×GliBS and 0.05 µg sv40-driven Renilla, together with or without 0.1 µg Crispr/Cas9 plasmids targeting Inversin. On the following day, the culture medium was changed to 0.5% serum-containing medium for 48 h to arrest the cells at the

G0 phase. Cells were then lysed, and the activity of Shh pathway was measured and normalized using the dual-luciferase reporter assay system (Promega, Cat. #E1960).

### **Reverse transcription-polymerase chain reaction (RT-PCR)**

In each sample,  $1 \times 10^6$  G0 phase cells were washed with the PBS buffer once and lysed with 1 ml TRIzol (Invitrogen, Cat. # 15596018) for 5 min at room temperature. The lysed cells were mixed sufficiently with 250  $\mu$ l trichloromethane, followed by centrifugation at 12,000 rpm for 15 min at 4 °C. The supernatants were mixed with equal volume of isopropanol, centrifuging at 12,000 rpm for 10 min to obtain the RNA precipitation. After washing with 75% ethyl alcohol, RNA was resuspended with 100  $\mu$ l RNase-free water. RNA concentration was measured and 1  $\mu$ g RNA was reversely transcribed using M-MLV reverse transcriptase (Invitrogen, Cat. # 28025021). The synthesis of Ptc1 and  $\beta$ -Actin was detected using primers: 5'-ATGGCCTCGGCTGGTAACGC-3' and 5'-CACAGCGAAGGCCCAAATA-3' for Ptc1; 5'-CCTGTGCTGCTCACCGAGGC-3' and 5'-CGGCAGTGGCCATCTCCTGC-3' for  $\beta$ -Actin.

### **Statistical analysis**

Statistical analysis was performed using Microsoft Office Excel 2016. We selected at least 150 samples in total in each of our experiment to achieve an adequate power  $> 0.8$ . P-values were calculated by the paired t-test from the mean values of the data. Significant differences were marked with asterisks (\*\* $p < 0.01$ , \*\*\* $p < 0.001$ ).

## Supporting Figures and Figure Legends

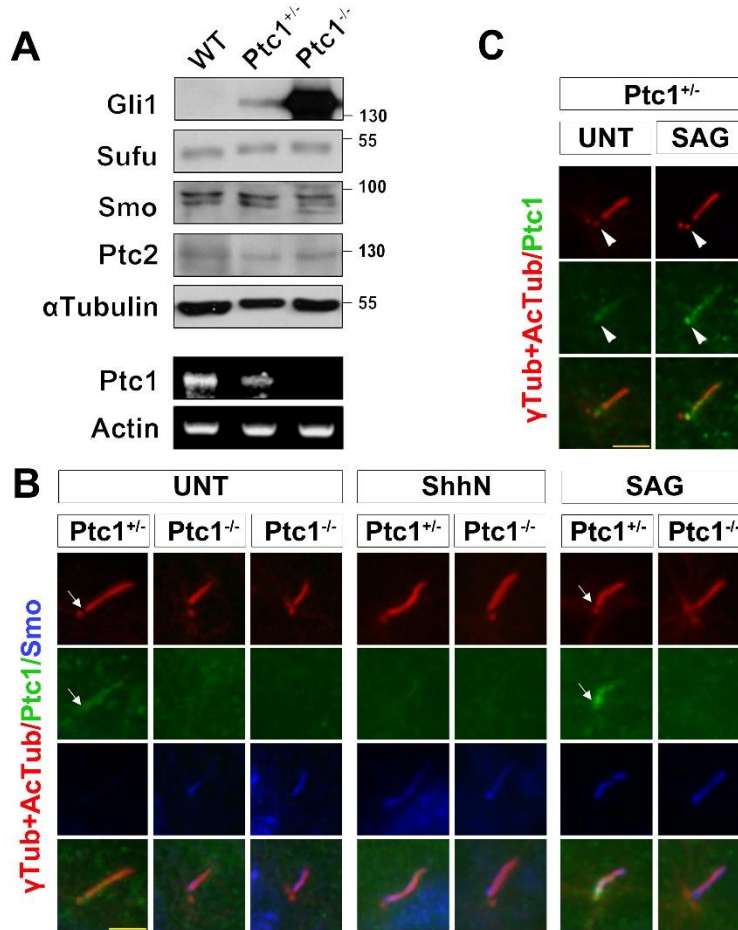


**Fig S1. Validation of the Ptc1<sup>-/-</sup> cells.** (A) Protein expression patterns in wild-type (WT), Ptc1<sup>+/-</sup>, and Ptc1<sup>-/-</sup> MEF cells. G0 phase MEF cells were examined for the expression of the indicated proteins. RT-PCR was used to verify WT, Ptc1<sup>+/-</sup>, and Ptc1<sup>-/-</sup> cells. (B, C) Validation of the Ptc1<sup>-/-</sup> cells by immunofluorescence, and a portion of Ptc1 localizes at the centrosome. G0 phase Ptc1<sup>+/-</sup> and Ptc1<sup>-/-</sup> MEF cells were immunostained for Ptc1, Smo,  $\gamma$ -Tubulin ( $\gamma$ Tub) and AcTub under the indicated treatment. Note that Ptc1 showed localization both inside the cilium and at the ciliary base (arrows in B, arrowhead in C) in Ptc1<sup>+/-</sup> cells, but not in Ptc1<sup>-/-</sup> cells. Scale bar, 5  $\mu$ m.

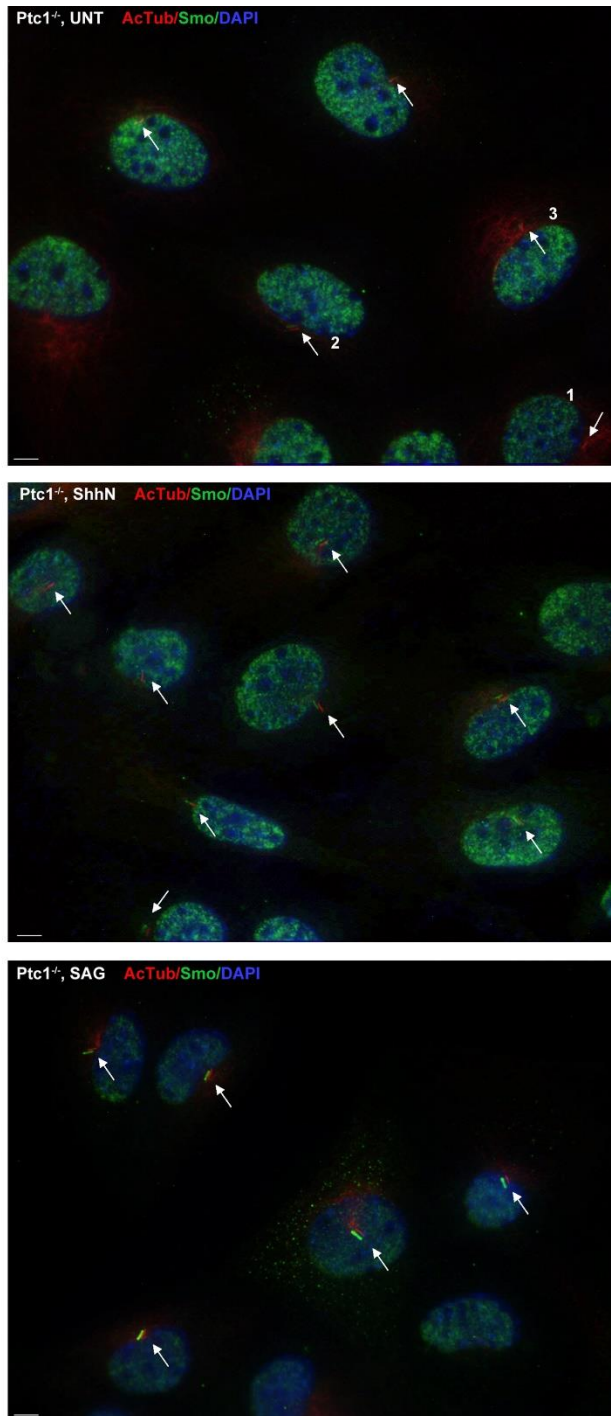


**Fig S2. Large view of the  $Ptc1^{-/-}$  cells, under untreated (UNT), ShhN-treated, or SAG-treated conditions.** G0 phase  $Ptc1^{-/-}$  cells under the indicated treatment were immunostained for Smo and AcTub. The green channel was shifted to make it easy to compare between the channels. Cilia are indicated by arrows. The Smo patterns in the current study were defined as no ciliary localization (cell #1), entire ciliary localization (cell #2), or localization at the ciliary proximal end (cell #3). Note that SAG treatment resulted in a strong, (universally) even, ciliary signal of Smo, but ShhN treatment resulted in a mild, (in most cases) even, ciliary signal of Smo. Scale bar, 10  $\mu$ m.

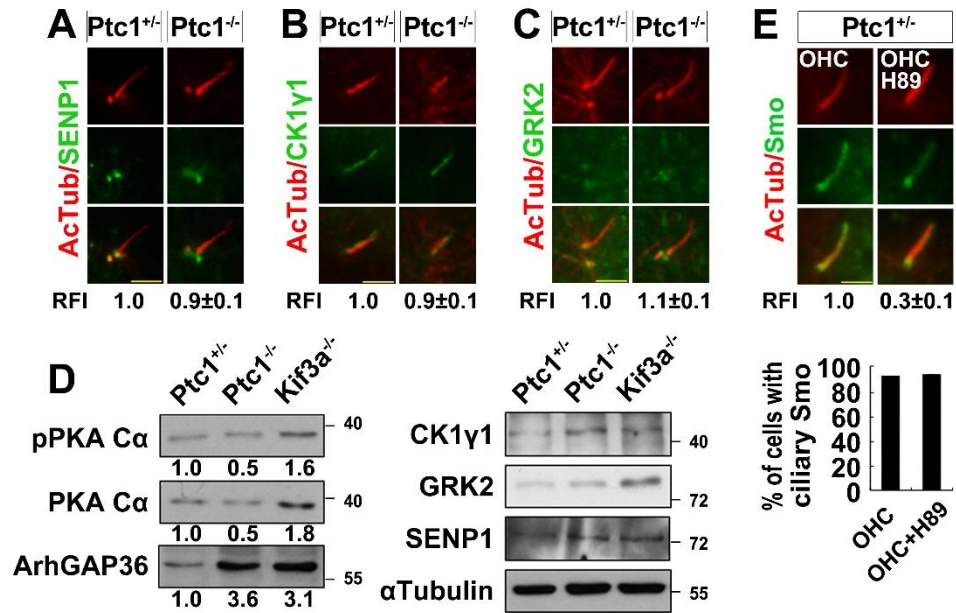


**Fig S3. Expression and localization of SENP1, CK1γ1, and GRK2 are not affected by Ptc1 knockout, and inhibition of PKA activity does not block the 20-OHC-induced Smo ciliary translocation.** (A-C) The centrosomal localization of SENP1 and GRK2, and the ciliary localization of CK1γ1 were similar in Ptc1<sup>+/+</sup> and Ptc1<sup>-/-</sup> cells. G0 phase Ptc1<sup>+/+</sup> and Ptc1<sup>-/-</sup> cells were immunostained for the indicated proteins. (D) Expression patterns of the indicated proteins in Ptc1<sup>+/+</sup>, Ptc1<sup>-/-</sup>, and Kif3a<sup>-/-</sup> cells. Note that the expression of ArhGAP36 and PKAc were negatively co-related with each other in Ptc1<sup>+/+</sup> and Ptc1<sup>-/-</sup> cells. The normalized results of PKAc, phosphorylated PKAc, and ArhGAP36 were shown below each panel, and the amount of the indicated proteins in Ptc1<sup>+/+</sup> cells was set as 1.0. (E) PKA activity has little effect on 20-OHC-induced Smo ciliary translocation. G0 phase Ptc1<sup>+/+</sup> cells were treated with 20-OHC (OHC), in the presence or absence of PKA inhibitor H89, and immunostained for the indicated proteins. The ratio of cells with ciliary Smo were shown below. The quantified relative fluorescence intensity (RFI) of the indicated proteins was shown below each panel. Scale bars, 5 μm.

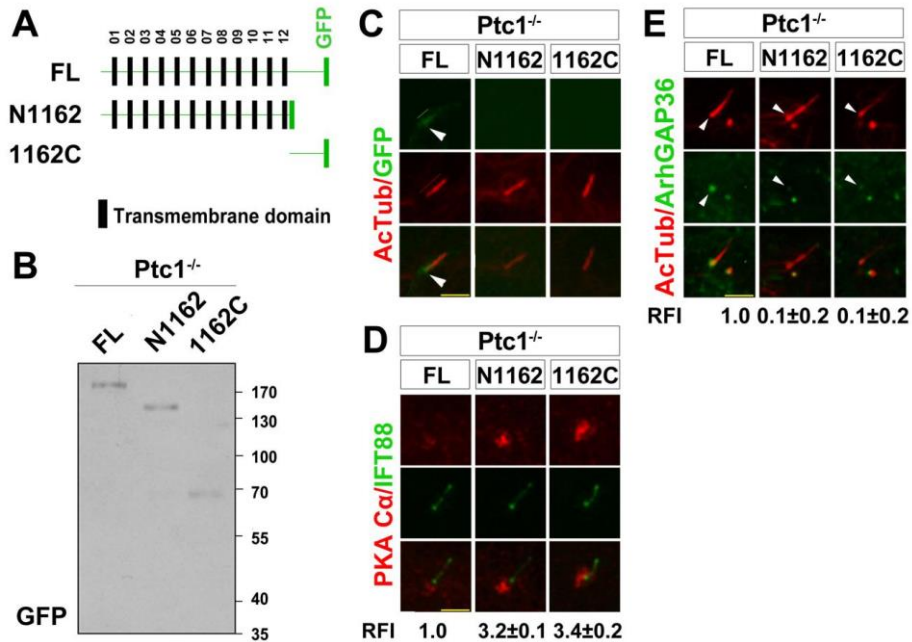


**Fig S4. Only full-length Ptc1 can inhibit PKAc accumulation at the centrosome.** (A) A cartoon showing the full-length and truncated form of Ptc1-GFP. N1162, the 1-1162 amino acids of Ptc1, which contains the intact 12 transmembrane domains; 1162C, the 1162-end amino acids of Ptc1, which contains the intact cytoplasmic tail of Ptc1. (B) Verification of full-length or truncated Ptc1-GFP stably expressing Ptc1<sup>-/-</sup> cells. The indicated Ptc1 proteins were introduced into Ptc1<sup>-/-</sup> cells by lentivirus to obtain weak expression levels, and the cells stably expressing these Ptc1 proteins were verified by Western blotting and cloned for further study in this paper. (C) Ptc1<sup>FL</sup> localizes to the ciliary proximal region. Stable cell-lines established from (B) were arrested at the G<sub>0</sub> phase, and immunostained for AcTub. The green and red lines each indicated the distribution of Ptc1<sup>FL</sup> shown by GFP and the axoneme labeled by AcTub. (D) Only Ptc1<sup>FL</sup> can inhibit PKAc accumulation at the centrosomes in Ptc1<sup>-/-</sup> cells. Stable cell-lines established from (B) were arrested at the G<sub>0</sub> phase, and immunostained for PKAc and IFT88. Scale bar, 5 μm. RFI was shown below each panel. (E) Only full-length Ptc1 stabilizes ArhGAP36 at the mother centriole. Stable cell-lines established from (B) were arrested at the G<sub>0</sub> phase, and immunostained for ArhGAP36 and AcTub.



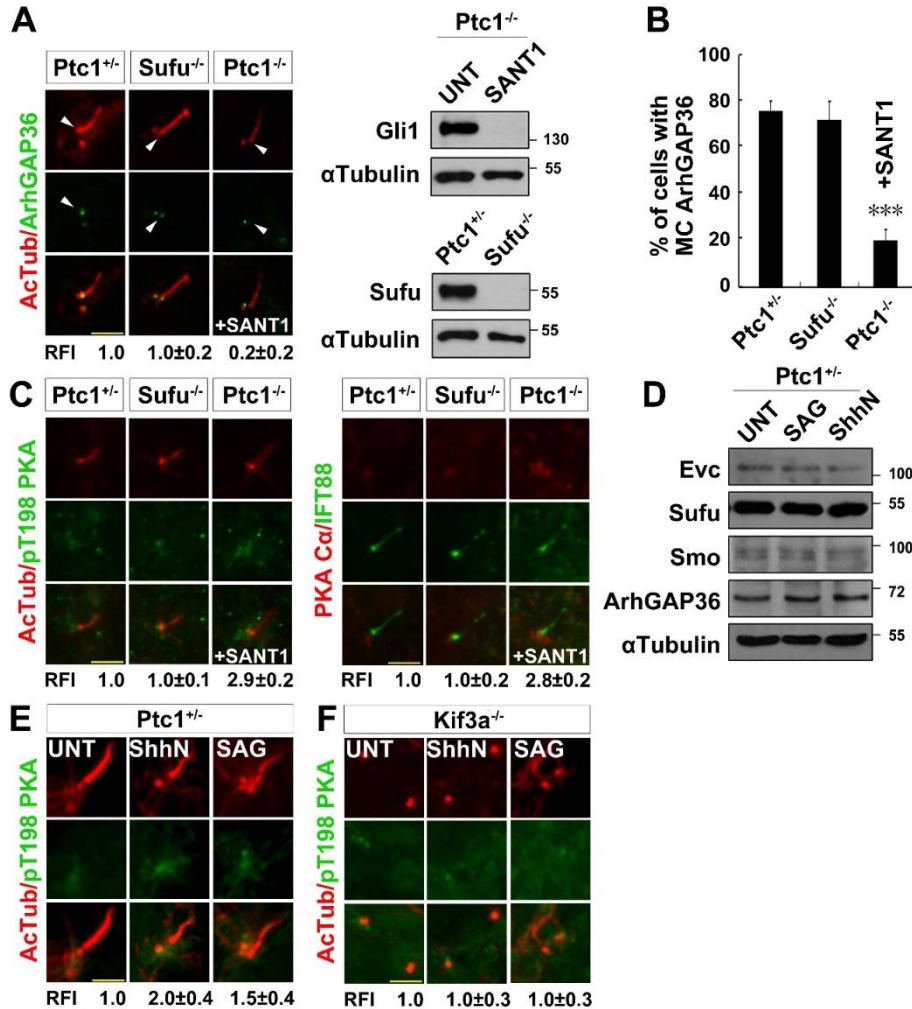


**Fig S5. Ptc1 but not Shh pathway activation by Glis determines the mother centriolar localization of ArhGAP36 and PKAc, and Shh pathway activation does not influence the protein level of ArhGAP36.** (A) ArhGAP36 localizes to the mother centriolar in *Sufu*<sup>-/-</sup> cells, and the inhibition of Shh pathway cannot restore the mother centriolar localization of ArhGAP36 in *Ptc1*<sup>-/-</sup> cells. G0 phase *Sufu*<sup>-/-</sup> or *Ptc1*<sup>-/-</sup> cells were immunostained for the indicated proteins. RFIs were shown below each panel. Inserts, validation of the *Sufu*<sup>-/-</sup> cells and of the inhibition of Shh pathway by SANT1. (B) The ratio of cells with mother centriolar ArhGAP36 in (A) was shown. (C) The centrosomal accumulation of PKAc depends on Ptc1 but not Shh pathway activation by Gli. G0 phase *Ptc1*<sup>+/-</sup>, *Sufu*<sup>-/-</sup> or SANT1-treated *Ptc1*<sup>-/-</sup> cells were immunostained for the indicated proteins. (D) Shh signaling has no effect on ArhGAP36 expression. G0 phase *Ptc1*<sup>+/-</sup> cells under SAG or ShhN treatment were examined for the expression of the indicated proteins. (E) Ptc1 inhibition by Shh signaling results in phosphor-PKAc accumulation at the centrosome. G0 phase *Ptc1*<sup>+/-</sup> cells under SAG or ShhN treatment were immunostained for AcTub and phosphor-T198 of PKAc. (F) Centrosomal PKAc accumulation by Shh signaling is cilium-dependent. G0 phase *Kif3a*<sup>-/-</sup> cells under SAG or ShhN treatment were immunostained for AcTub and phosphor-T198 of PKAc. Note that the amounts of centrosomal phosphor-PKAc did not change under Shh pathway activation in *Kif3a*<sup>-/-</sup> cells. RFIs were shown below each panel. Scale bar, 5 μm.

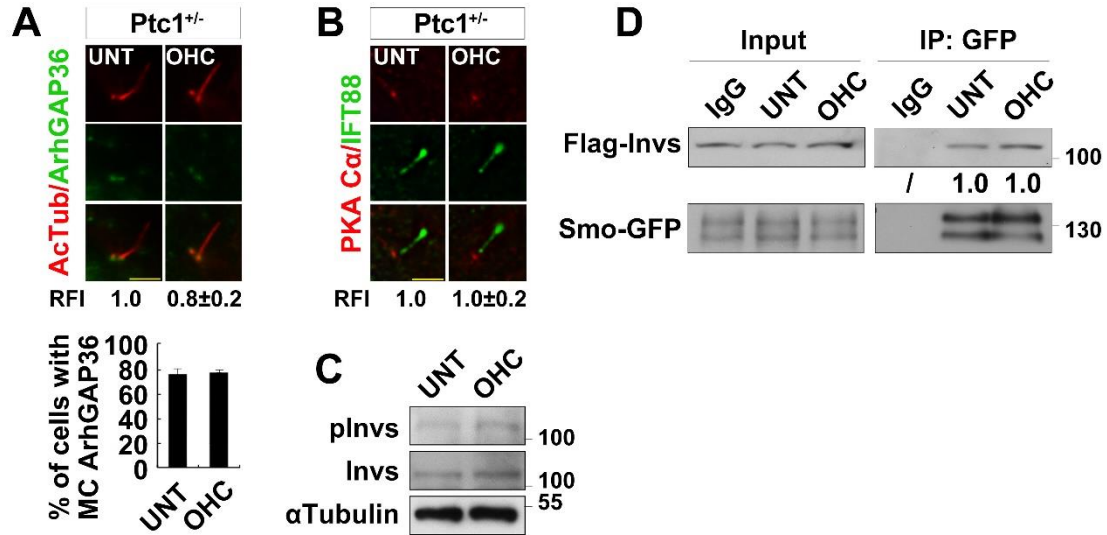


**Fig S6. The ciliary translocation of Smo by 20-OHC is irrelevant to the PKA-Inversin axis.** (A, B) 20-OHC treatment has little effect on regulating the amount of centrosomal ArhGAP36 and PKAc. G0 phase *Ptc1<sup>+/-</sup>* cells were treated or untreated with 20-OHC, and immunostained for the indicated proteins. RFIs are shown below each panel. Scale bar, 5  $\mu$ m. (C) 20-OHC treatment does not result in Inversin phosphorylation. G0 phase *Ptc1<sup>+/-</sup>* cells were treated or not treated with 20-OHC, followed by Western blot. (D) 20-OHC treatment does not increase the interaction between Inversin and Smo. HEK 293T cells were co-transfected with the indicated plasmids, arrested at the G0 phase, treated or not treated with 20-OHC, and followed by an IP assay. The normalized results of immunoprecipitated Inversin were shown below each panel, and the amount of Inversin in UNT was set as 1.0.

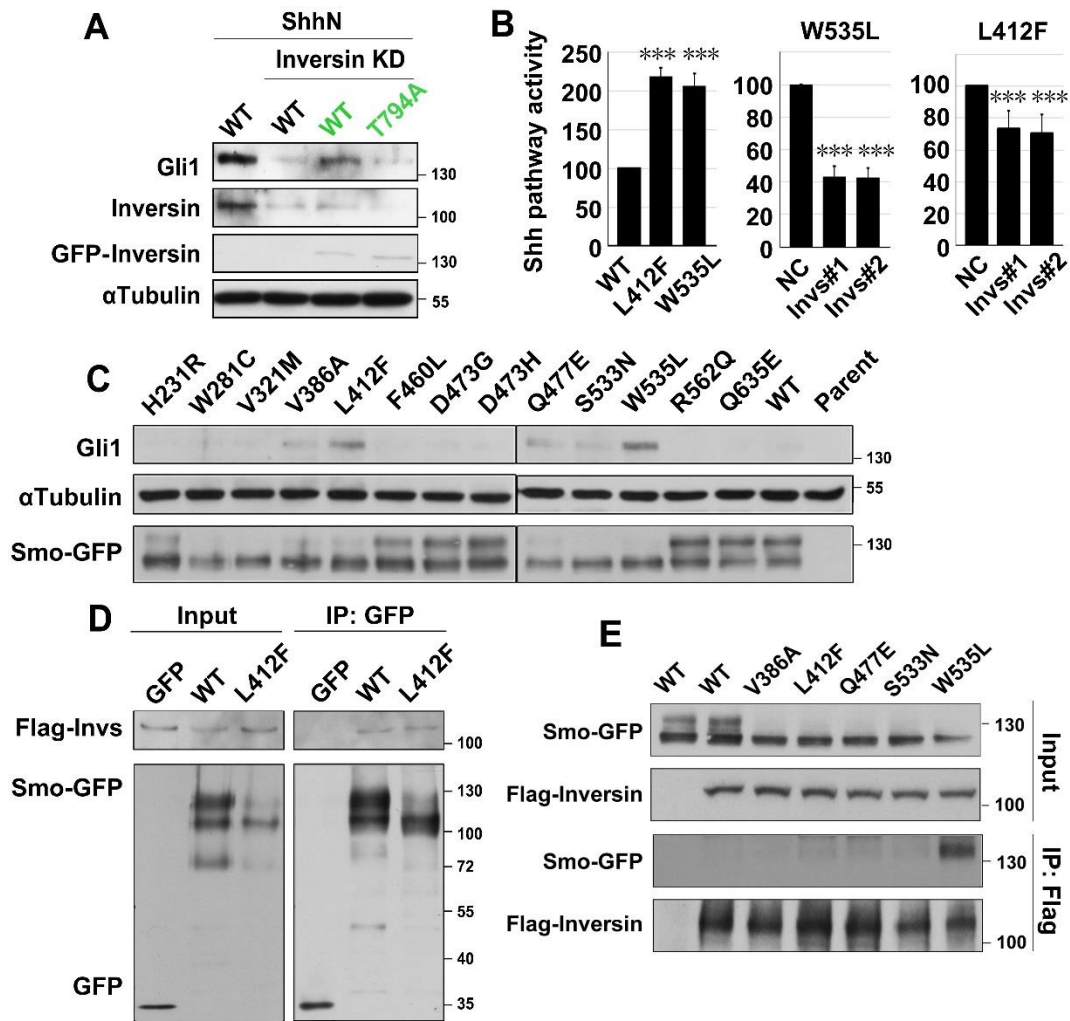


**Fig S7. The mechanism of Shh pathway activation in Smo<sup>L412F</sup>- and Smo<sup>L412F</sup>-driven tumor cells might be different.** (A) Shh signaling is mediated by Inversin in a PKA phosphorylation-dependent manner. The WT MEF cells, or the two MEF cell-lines stably carrying GFP-Inversin<sup>WT</sup> or GFP-Inversin<sup>T794A</sup> were knocked down for Inversin, and treated with ShhN. The expression of the indicated proteins was examined. (B) Shh pathway activity is significantly decreased by Inversin knockdown in Smo<sup>W535L</sup>-expressing cells. The indicated cell-lines were transfected with the luciferase reporter, arrested at the G0 phase, knocked down for Inversin, and the activity of Shh pathway in each cell-line was examined. (C) Smo mutants stimulate Shh pathway with different ability. Cells were arrested at the G0 phase and examined for the indicated proteins. (D) The Smo<sup>L412F</sup> mutant does not show increased binding with Inversin. HEK 293T cells were co-transfected with the indicated plasmids, arrested at the G0 phase, followed by an IP assay. (E) The Smo<sup>W535L</sup> mutant binds Inversin with a high ability. HEK 293T cells were co-transfected with the indicated plasmids and arrested at the G0 phase, followed by an IP assay.

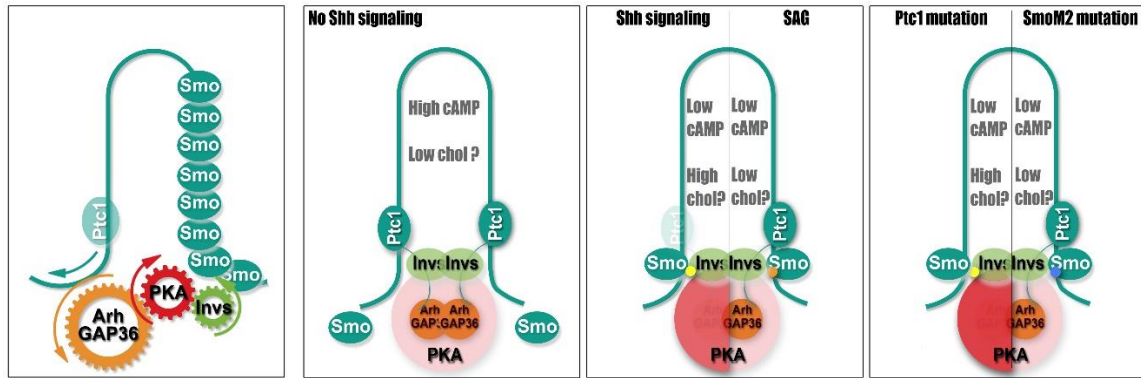
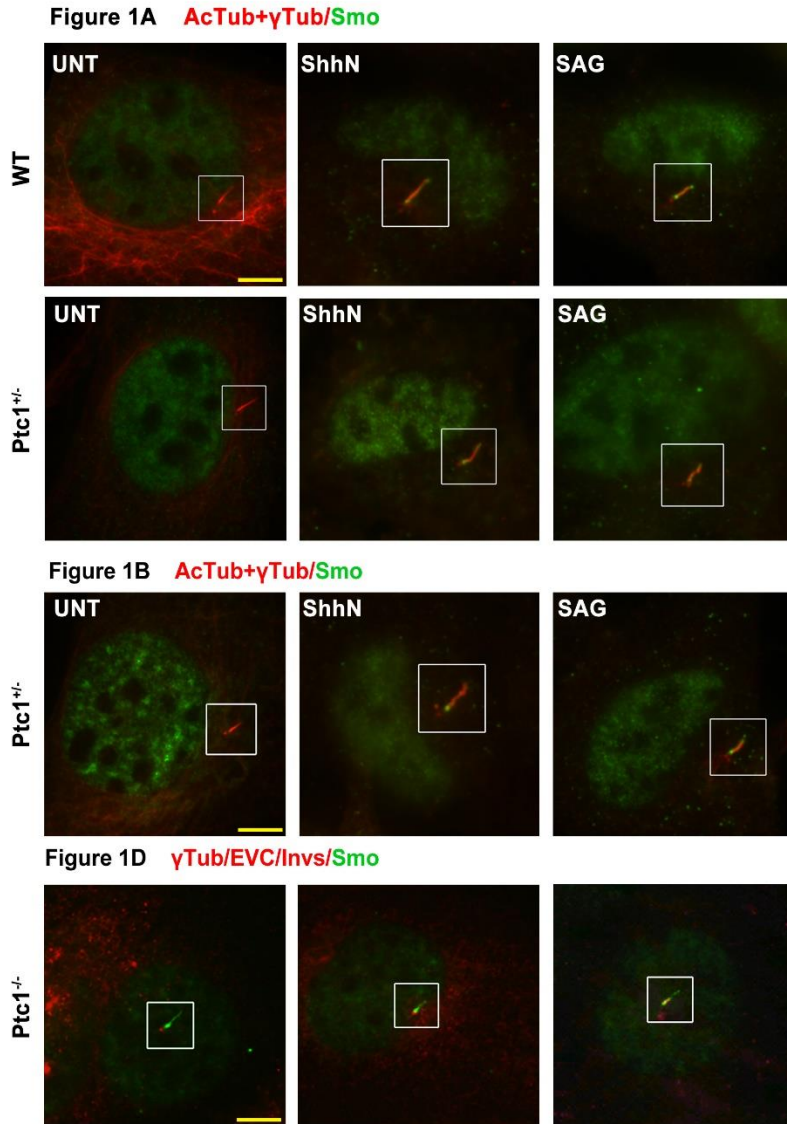


**Fig S8. A working model illustrating how Ptc1 inhibits the ciliary translocation of Smo and how Smo is de-repressed during the initiation of Shh pathway activation.** The left cartoon shows how the Ptc1-ArhGAP36-PAK-Inversin-Smo cascade works. The right three cartoons show how the activity and ciliary translocation of Smo is regulated by Ptc1 under normal and oncogenic mutation conditions. In the absence of the Shh ligand, Ptc1 interacts with ArhGAP36 *via* its cytoplasmic tail and stabilizes ArhGAP36 at the mother centriole, resulting in a low amount of centrosomal PKAc and low kinase activity of PKA. At this stage, the level of ciliary cAMP is high and (possibly) the level of ciliary cholesterol (chol) is low, leading to high kinase activity of ciliary PKA, which mediates the proteolytic processing of Gli, and low activity of ciliary Smo, if any. Under Shh pathway activation state, the ciliary translocation of Smo promotes the exit of ciliary Gpr161 and accordingly decreases the kinase activity of ciliary PKA, which suspends the proteolytic processing of Gli. The difference between Shh ligand- and SAG-induced pathway activation is whether the ciliary translocation of Smo relies on the increased kinase activity of centrosomal PKA – the Shh ligand drives Smo translocation into the cilium *via* increasing the amount of phosphorylated Inversin (yellow circle), whereas SAG does this *via* inducing a conformation of Smo (golden circle). Under oncogenic mutation conditions, the loss-function mutations of Ptc1 mimic when the Shh ligand binds with it under normal conditions, whereas the W535L mutation of Smo increases its binding with Inversin *via* inducing a specific conformation of Smo (blue circle). Both SAG treatment and the W535L mutation of Smo can bypass the inhibitory effect of Ptc1 *via* interacting with Inversin / localizing at the ciliary proximal region to initiate Shh pathway activation.

**Fig S9. Full images underlying the cropped regions shown in the related figures.** The full images are listed with the same order as they are shown in each figure. To orient all the cilia toward 2 o'clock in this paper, some of the original images were rotated. White lines indicate the margin(s) of the original images. Scale bars, 10  $\mu$ m.

*Full images for Figure 1*



Full images for Figure 2

Figure 2A PKAc/IFT88

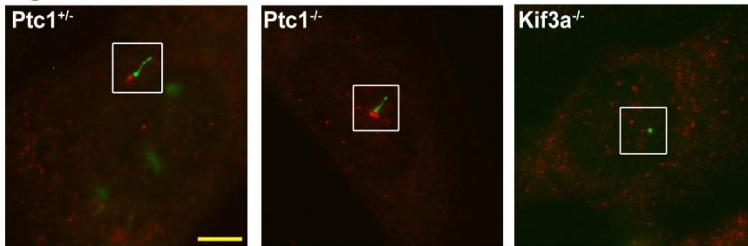


Figure 2B AcTub/pT198 PKAc

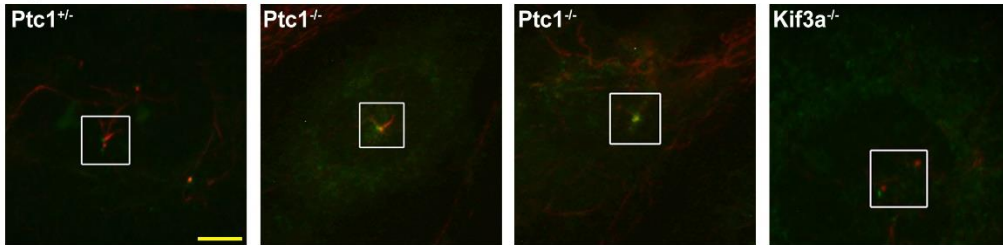


Figure 2D AcTub/Smo

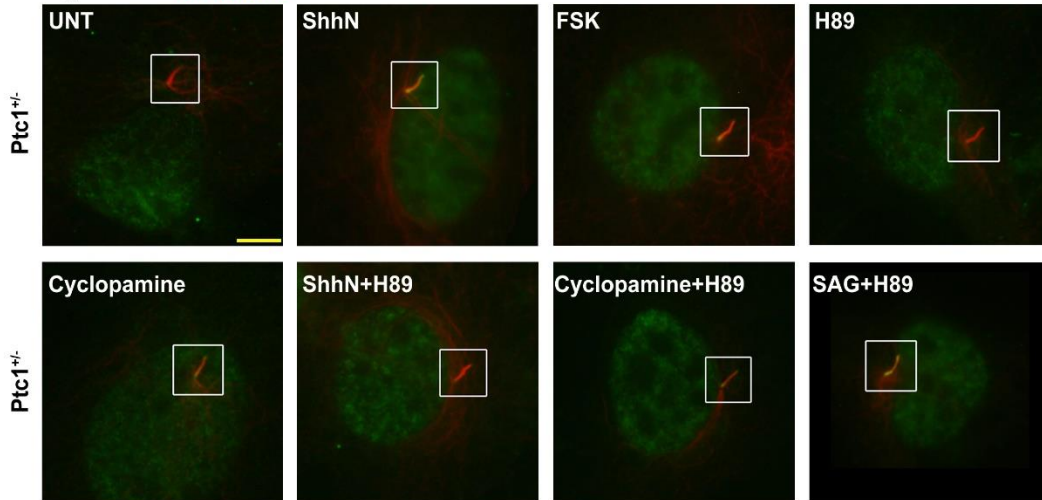


Figure 2F AcTub/Smo

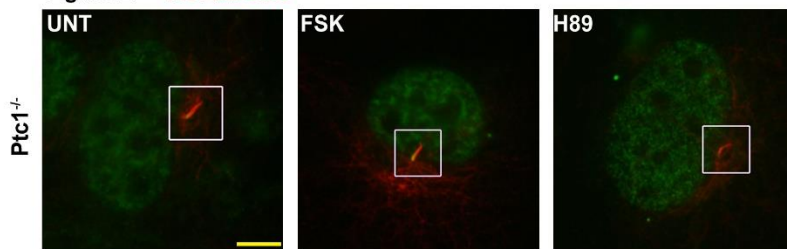
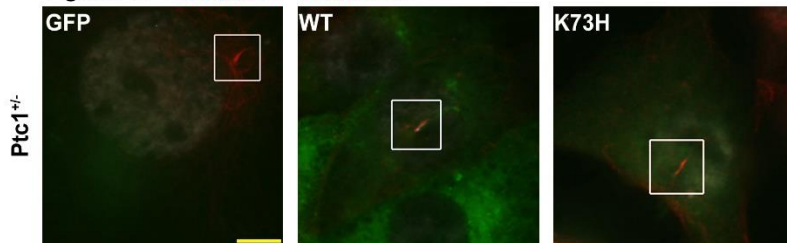


Figure 2H AcTub/GFP-PKAc/Smo



*Full images for Figure 3*

Figure 3A **AcTub/ArhGAP36**

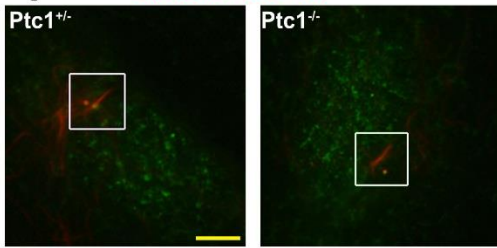


Figure 3C **PKAc/GFP-CLS/ArhGAP36**

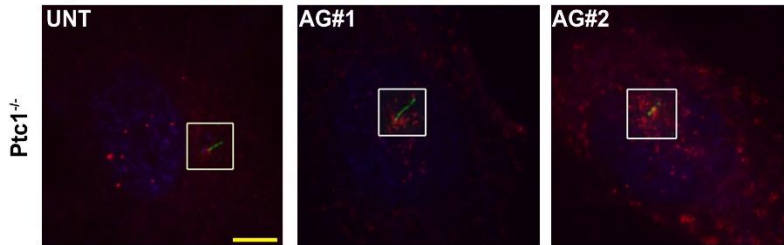


Figure 3D **AcTub/Smo**

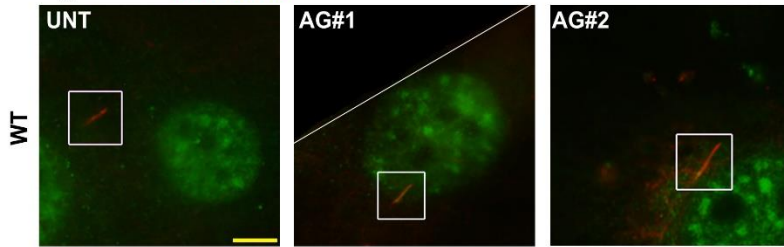


Figure 3E **AcTub/ArhGAP36**

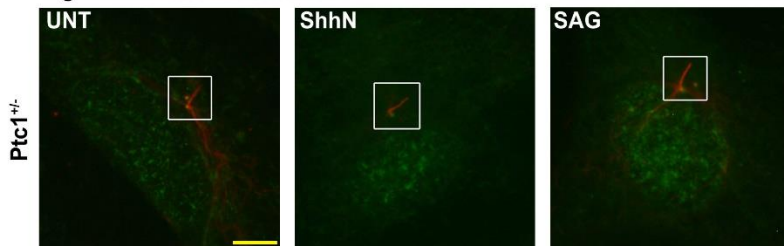
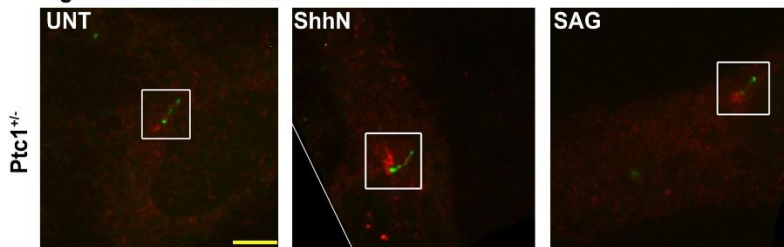
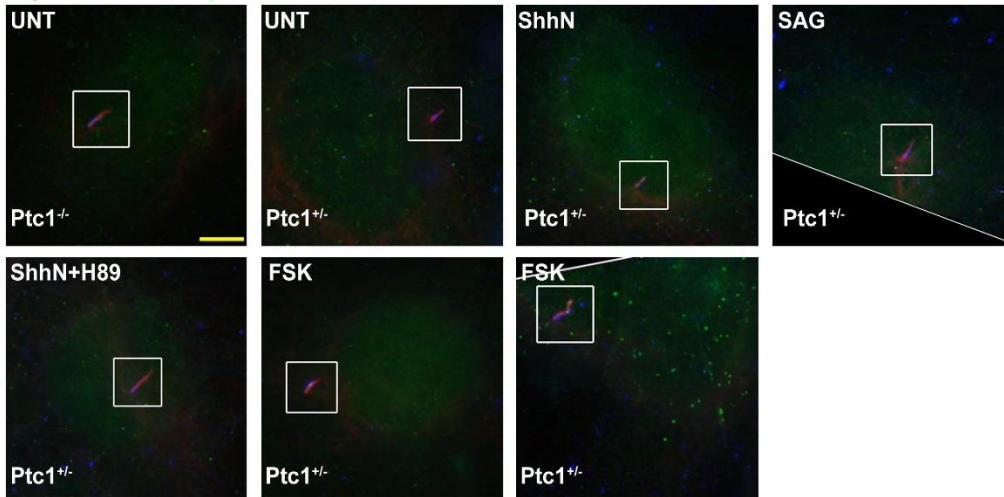


Figure 3F **PKAc/IFT88**



*Full images for Figure 4*

Figure 4E **AcTub/plnvs/lnvs**



*Full images for Figure 5*

Figure 5B **PLA/AcTub**

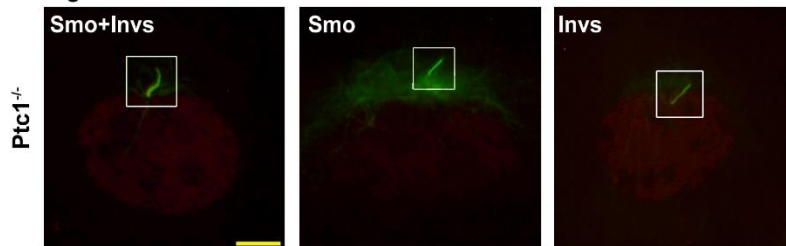
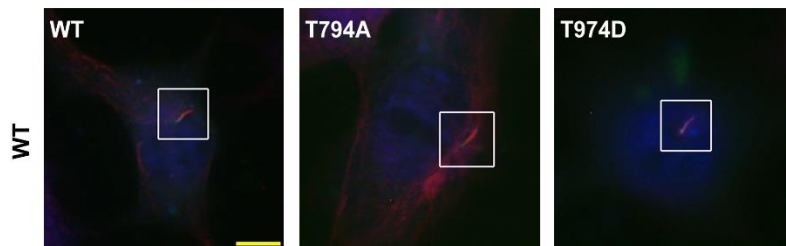
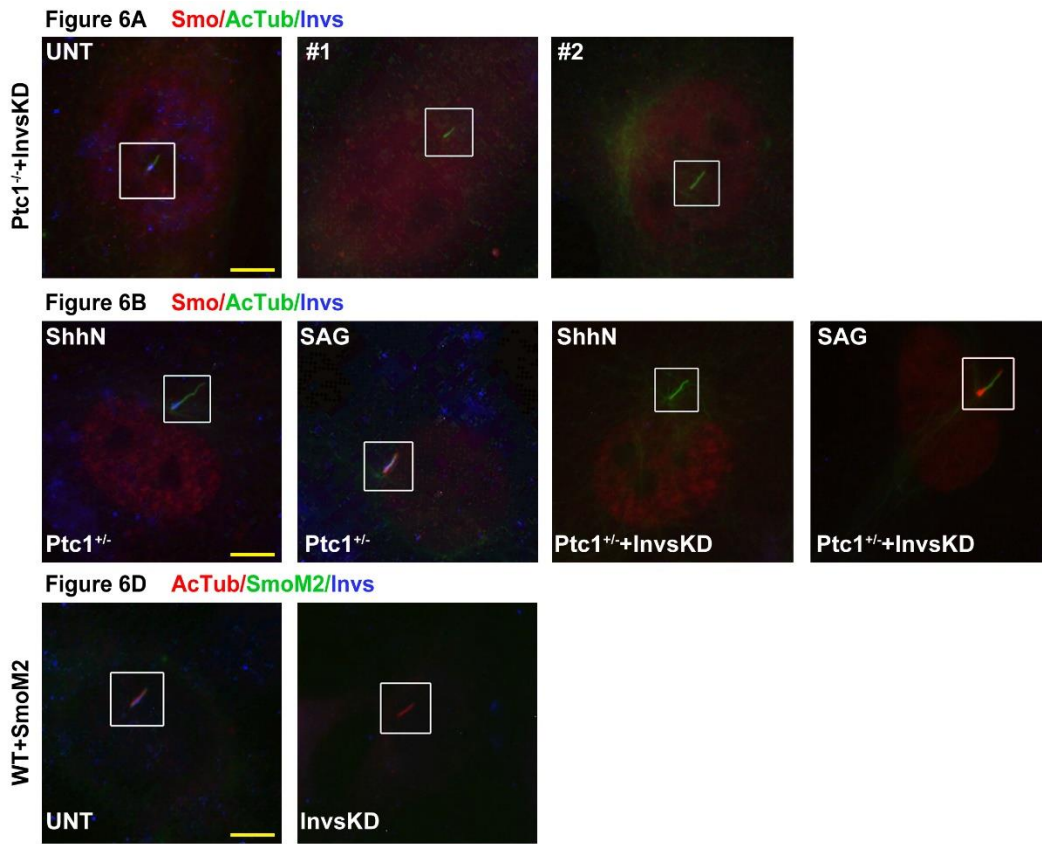


Figure 5C **AcTub/GFP-Inversin/Smo**





Full images for Figure 6



*Full images for Figure S1*

Figure S1B **AcTub+ $\gamma$ Tub/Ptc1/Smo**

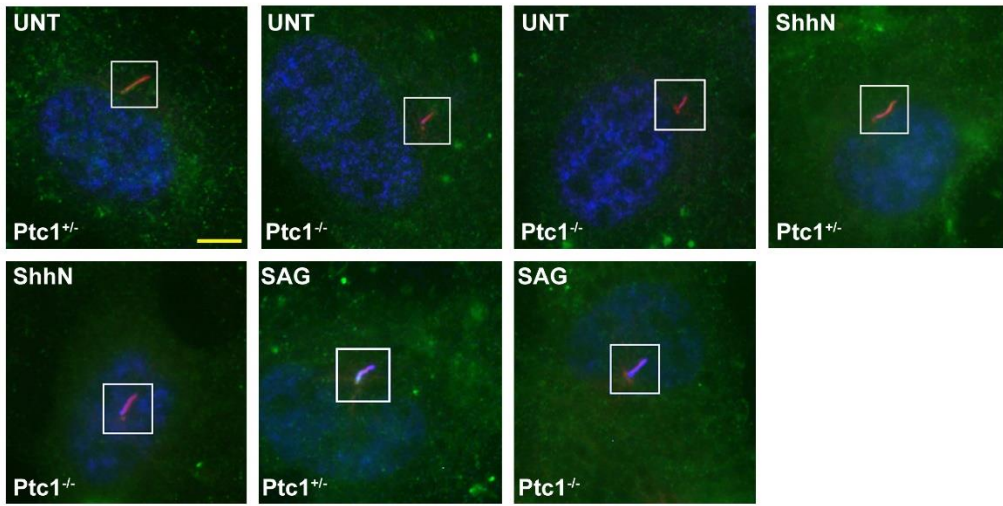
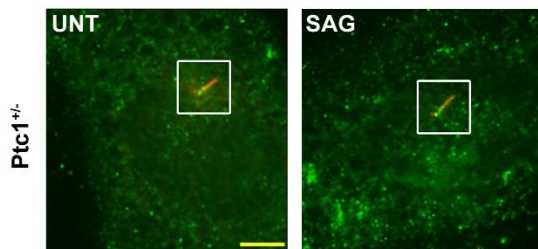


Figure S1C **AcTub+ $\gamma$ Tub/Ptc1**



*Full images for Figure S3*

Figure S2A **AcTub/SENP1**

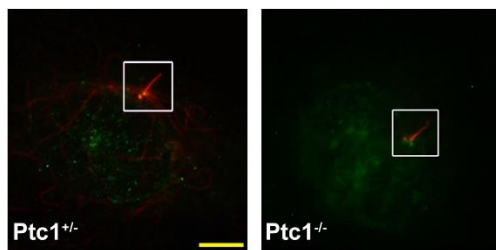


Figure S2B **AcTub/CK1 $\gamma$ 1**

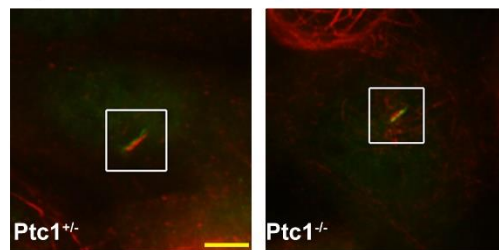


Figure S2C **AcTub/GRK2**

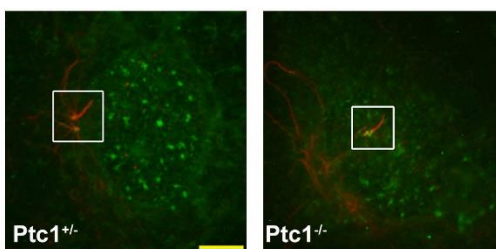
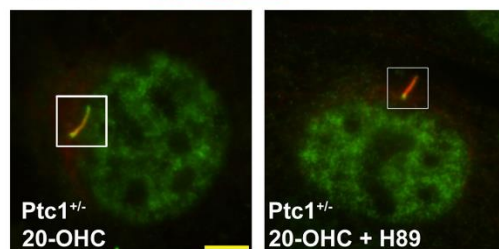


Figure S2E **AcTub/Smo**



*Full images for Figure S4*

Figure S3C **AcTub/GFP**

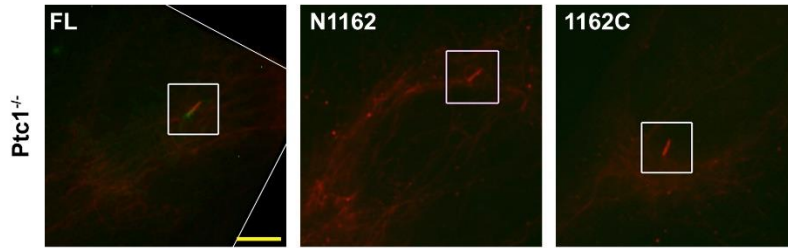


Figure S3D **PKAc/IFT88**

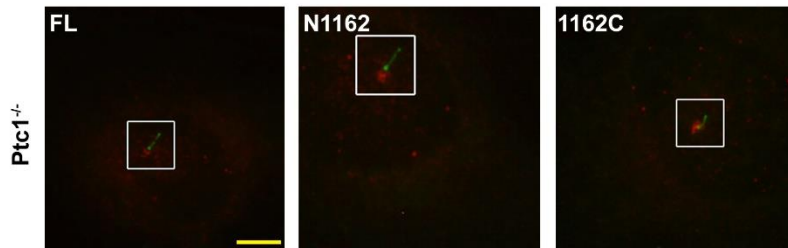
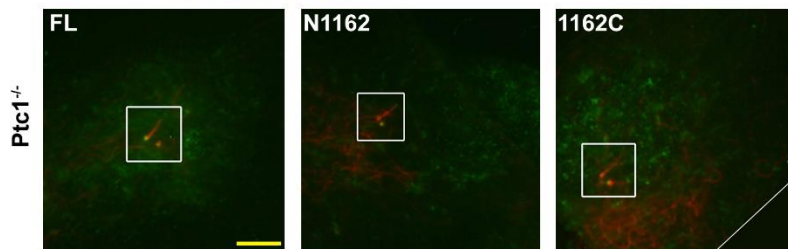


Figure S3E **AcTub/ArhGAP36**



Full images for Figure S5

Figure S4A AcTub/ArhGAP36

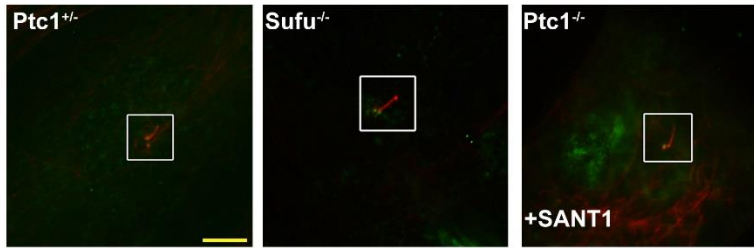
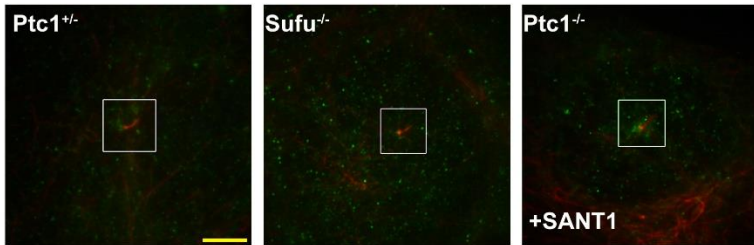


Figure S4C AcTub/pT198 PKAc



PKAc/IFT88

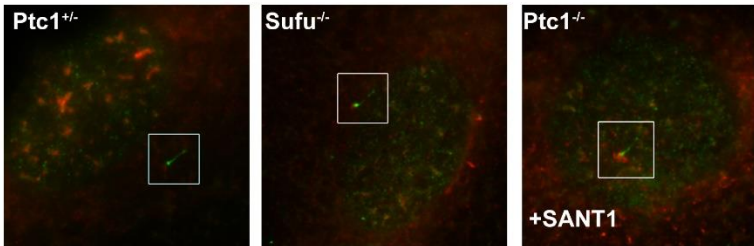


Figure S4E AcTub/pT198 PKAc

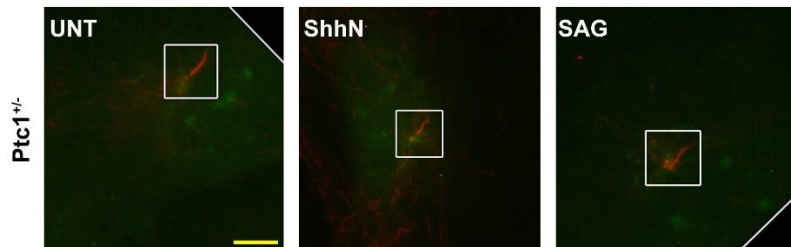
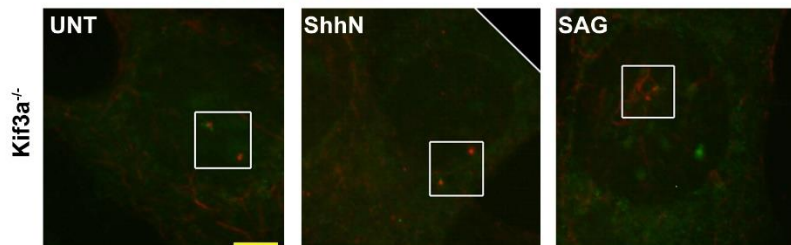


Figure S4F AcTub/pT198 PKAc



*Full images for Figure S6*

